

RESEARCH

Open Access



Microwave-assisted synthesis and dual in silico–in vitro profiling of vanillin azo-Schiff base hybrids for antimicrobial potential

Mohamad Azmeer Hissam^{1*}, Zainab Ngaini^{1*}, Nur Arif Mortadza², Adibah Izzati Daud³ and Saba Farooq⁴

*Correspondence:

Mohamad Azmeer Hissam
24010130@siswa.unimas.my
Zainab Ngaini
nzainab@unimas.my

¹Faculty of Resource Science and Technology, Universiti Malaysia Sarawak, 94300 Kota Samarahan, Sarawak, Malaysia

²Faculty of Agrotechnology and Applied Sciences, i-CATS University College, 93350 Kuching, Sarawak, Malaysia

³Faculty of Chemical Engineering and Technology, Universiti Malaysia Perlis, 02600 Arau, Perlis, Malaysia

⁴Department of Basic and Applied Chemistry, Faculty of Science and Technology, University of Central Punjab, Lahore 54000, Pakistan

Abstract

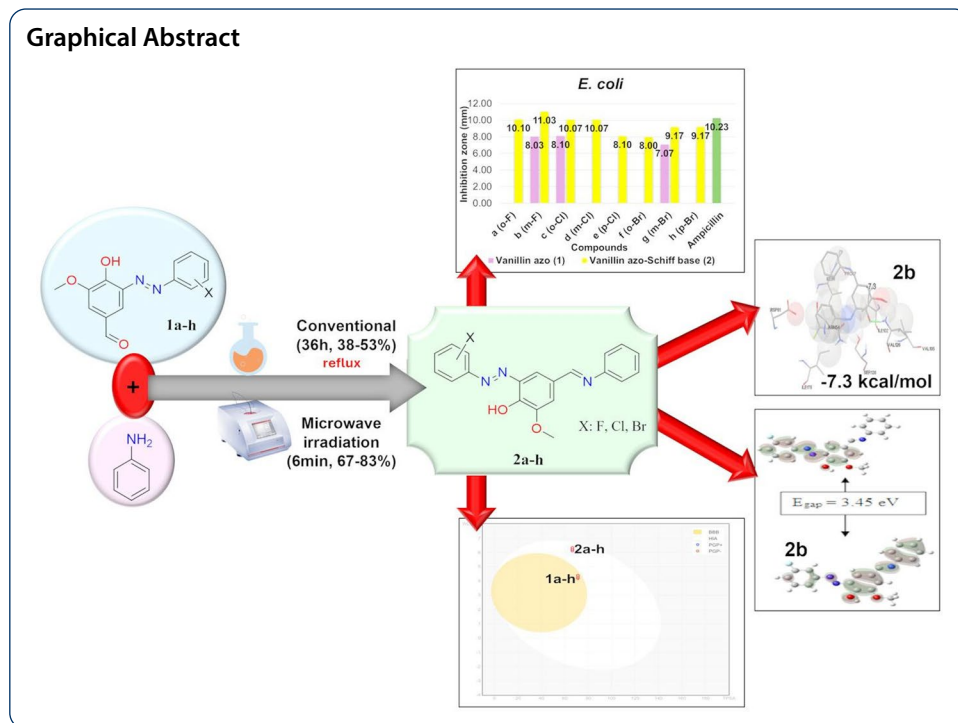
Researchers have demonstrated substantial interest in bioactive compounds derived from natural resources, such as vanillin, owing to their significant potential in drug development. Here, we report the efficient synthesis of hybrid azo-Schiff bases derived from vanillin **2(a–h)** using vanillin azo **1(a–h)** as natural product-based precursors, achieved *via* microwave irradiation to yield significant amounts (67–83%, 6 min) compared to conventional heating (38–53%, 36 h). Compounds **2(a–h)** exhibited enhanced antibacterial activity against *S. aureus* (inhibition zones of 9–11 mm) compared to **1(a–h)** (7–9 mm) and the parent vanillin, which showed no inhibition. Similarly, **2(a–h)** demonstrated superior activity against *E. coli* (8–11 mm) relative to **1(a–h)** (7–9 mm) and vanillin (no inhibition). Compound **2b** exhibited the most potent antibacterial activity among the synthesised compounds, with inhibition zones of 11.03 ± 0.12 mm against *E. coli* and 11.20 ± 0.10 mm against *S. aureus*, comparable to the standard antibiotic ampicillin (11–12 mm). Compound **2b** also revealed a strong binding affinity of -7.3 kcal/mol in molecular docking analysis, alongside an energy gap of 3.45 eV as determined by DFT calculations using Gaussian 09, indicating favourable electronic properties for antimicrobial activity. The ADMET studies supported natural product-based hybrids derived from vanillin as suitable drug candidates. This research significantly advances drug design by presenting potent in vitro antibacterial agents derived from natural products, characterised by promising pharmacological and physicochemical properties.

Keywords Absorption, Binding energy, DNA gyrase enzyme, Energy gap, Halogen.

1 Introduction

Multidrug-resistant superbugs pose a critical global health crisis, necessitating urgent and comprehensive strategies to effectively combat antimicrobial resistance (AMR). Pathogenic infections are responsible for an estimated 7.7 million deaths, with *S. aureus* and *E. coli* identified as primary bacterial pathogens driving this alarming trend [1]. Despite active research into effective therapeutic strategies to combat AMR, the substantial costs and intricate processes inherent in developing new drugs remain major obstacles [2]. To overcome these hurdles, the exploration of chemical modification





strategies applied to natural product-based compounds has garnered significant interest due to their considerable potential for drug development and therapeutic applications [3]. Vanillin is a bioactive compound that can be extracted from vanilla beans and is widely utilised in food-grade additives [4] and medicines [5]. Building on this, researchers have increasingly turned to synthetic approaches involving the chemical modification of these natural resources with active scaffolds, aiming to enhance their effectiveness and optimise interactions with biological targets [6]. A notable success in structural modification of vanillin is Trimethoprim, one of the commercially available antibiotics to combat bacterial infections [7].

Recent advancements in the functionalization of vanillin have demonstrated its potential as a versatile scaffold for the development of bioactive compounds. The structural modification of vanillin has gained interest within the scientific community to develop compounds with diverse biological activities, including anticancer [8–10], antiviral [11], antifungal [12] and antibacterial properties [13]. Among the various modifications, the incorporation of nitrogen-based moieties such as azo ($-N=N-$) and Schiff base ($-C=N-$) groups has garnered significant attention due to their distinct electronic properties and biological activities. Prior research, for instance, has underscored the significance of integrating these moieties into vanillin scaffolds, leading to vanillin-azo [14, 15] and vanillin Schiff bases [16, 17] that exhibit notably enhanced antimicrobial activities. This enhancement is often attributed to the synergistic effects between vanillin and these nitrogen chromophores, which can form crucial hydrogen bond interactions with the bacterial surface [18]. Generally, nitrogen chromophores are widely recognised for their crucial contribution in developing potent antibiotics such as nifuroxazide ($C=N$) and phenazopyridine ($N=N$) to treat bacterial infections [19, 20]. While Schiff base derivatives have shown superior antibacterial efficacy compared to azo analogues, particularly

against *Staphylococcus aureus* and *Escherichia coli* [18], many existing studies have examined these functional groups independently.

The strategic integration of both moieties within a single molecular scaffold remains insufficiently explored, despite its potential to enhance bioactivity through synergistic effects. In 2020, Kaur et al. developed a series of diazenyl Schiff base compounds and demonstrated their significant antimicrobial properties, alongside notable cytotoxic effects against the HCT-116 human colorectal carcinoma cell line. These findings highlight the therapeutic promise of such bifunctional molecular frameworks, particularly in the development of compounds with dual antimicrobial and anticancer potential [21]. This dual-functionalization strategy not only improves lipophilicity and electron delocalization but also enhances molecular interactions with bacterial targets. In contrast, a broader class of azo-Schiff base compounds has been reported, emphasising multifunctional applications in dyes, sensors and antimicrobial agents. Nevertheless, it was primarily on azobenzene systems and lacked specific insights into vanillin-based hybrids [22].

Encouraged by our recent findings on the excellent biological activity of vanillin hybrid compounds incorporating both azo (N=N) and chalcone (–C=C–) functionalities [23], we hypothesised that the integration of nitrogen-rich moieties could further enhance biological efficacy. This hypothesis is supported by the growing recognition that molecular hybridisation of natural products with structurally diverse pharmacophores offers a promising strategy for enhancing biological performance through synergistic interactions [6, 24]. Building upon this rationale, the present study focuses on the synthesis of novel vanillin-based hybrid compounds that combine both azo and Schiff base moieties, aiming to improve antimicrobial activity against *S. aureus* and *E. coli*.

Herein, we report the comparative synthesis of halogen-substituted vanillin azo-Schiff base hybrids **2(a–h)** via condensation of vanillin precursors **1(a–h)** with aniline, employing both microwave-assisted and conventional heating methods. The antibacterial activities of all synthesised compounds were evaluated against *S. aureus* (S48/81) and *E. coli* (ATCC 25922). In addition, computational analyses were conducted, including molecular docking to assess binding affinities, density functional theory (DFT) calculations to investigate electronic properties, and ADMET profiling to predict pharmacokinetic behaviour. These integrated approaches provide a comprehensive evaluation of the compounds' potential as antimicrobial agents.

2 Experimental

All chemicals used were of analytical grade and were utilised without further purification. Stuart MP3 apparatus was used to determine melting points via open tube capillary method. NMR spectra were recorded on a JEOL ECA 500 spectrometer (500 MHz for ^1H and 126 MHz for ^{13}C nuclei). Chemical shifts were referenced to DMSO- d_6 and reported in δ (ppm). Microwave-assisted synthesis was carried out using the Anton Paar Microwave Synthesis Reactor, Monowave 300. FTIR spectra were recorded using a PerkinElmer Thermo Scientific (Smart Omni Transmission Nicolet iS10 spectrophotometer).

2.1 Preparation of vanillin precursors **1(a–h)**

Vanillin precursors **1(a–h)** were prepared following previous literature [18]. NaNO_2 solution (2 M, 5 mL) was added to the halogenated aniline (5 mmol) in HCl (2 M, 10

mL) mixture while maintaining a temperature of 0–5 °C, followed by introducing vanillin (5 mmol) dissolved in NaOH solution (0.4 g, 10 mmol). Subsequently, HCl (2 M) was added to induce the formation of the precipitate upon completion of the reaction. Following filtration, the precipitate was recrystallised in ethanol to yield compounds **1(a–h)** [18]. Detailed characterisation data can be accessed through the supplementary file (Figures S2 and S3).

2.2 General synthesis of hybrid vanillin azo-Schiff base **2(a–h)**

2.2.1 Conventional heating

Compounds **2(a–h)** were synthesised following the previously reported method with slight modifications (e.g. solvents, temperature, times) [18]. Aniline (0.5 mmol) and azo precursor **1(a–h)** (0.5 mmol) were dissolved in methanol for 36 h at reflux conditions. Upon completion of the reaction, cold distilled water was added to precipitate the crude product. The crude obtained was filtered and recrystallised from hot methanol to yield compounds **2(a–h)**.

2.2.2 Microwave irradiation

An equimolar mixture of aniline (0.5 mmol) and azo intermediates **1(a–h)** (0.5 mmol) was subjected to microwave-assisted (700 W) in methanol (10 mL) at 170 °C for 6 min. Upon completion, cold distilled water was added to the mixture to induce precipitation. The crude precipitate was collected by filtration and subsequently recrystallised from hot methanol to yield the target compounds **2(a–h)**. Purity assessment and characterisation data for these compounds are provided in the supplementary files (Figures S2, S3, S4 and Table S1).

2.3 Antibacterial studies (*In vitro*)

The antimicrobial activities of compounds **1(a–h)** and **2(a–h)** towards *S. aureus* and *E. coli* were examined using the disc diffusion method (i.e., Kirby-Bauer) [18]. Ampicillin was used as the reference drug, while DMSO served as the negative control. All compounds (100 µg/mL) were dissolved in DMSO and applied to sterile paper discs before being placed on a microorganism-inoculated medium. The assay was performed in triplicate. Following 24 h of incubation, the diameters of the inhibition zones were measured and documented. The antibacterial activity of the target compounds is illustrated in the Supplementary file (Figure S1 and Table S2).

2.4 Statistical analysis

The antibacterial data are expressed as mean ± standard deviation (SD) and are available in the Supplementary Information (Table S1). The antibacterial activities of all compounds **1(a–h)** and **2(a–h)** were statistically evaluated using Welch's two-tailed t-test for unequal variances. Significant differences were observed for both bacterial strains, with *p*-values of 0.005 for *S. aureus* and *p* = 0.013 for *E. coli*. A *p*-value less than 0.05 was considered statistically significant.

2.5 Molecular docking analysis (*in silico*)

Docking of ligand-receptor complexes was analysed using AutoDock Tools and AutoDock Vina. The X-ray crystal structure of *S. aureus* Gyrase B 24 kDa in complex

with Novobiocin (PDB ID: 4URO) was retrieved from the Protein Data Bank. The active site was identified using AutoGridFR, and a cubic grid box of 25 Å was defined with a spacing of 0.5 Å, centred at coordinates $x=36.748$, $y=-13.829$, $z=9.075$ to encompass the active site region.

2.6 Pharmacokinetic studies

All compounds were evaluated for their potential as drug candidates and ADMET profile through SwissADME [25] and pkCSM [26] (Tables S3 and S4). These accessible online tools reduce reliance on empirical experimentation to determine prospective drug candidates for drug development [27]. In this study, Lipinski's rule was applied as a preliminary study to evaluate the drug-likeness of the synthesised compounds, complemented by computed ADMET properties to assess their pharmacokinetic profiles.

2.7 DFT method

The impact of various substituents' chemical reactivity on the synthesised compounds was investigated *via* DFT. Gaussian 09 [28] was used to analyse the geometric optimisation, and GaussView 5.0 [29] was employed to visualise the results. DFT calculations were performed using the B3LYP/6-311G(d, p) basis set. Frontier molecular orbital (FMO) analysis provided initial insights into the HOMO–LUMO energy levels, which were used to derive key reactivity descriptors including energy band gap (E_{gap}), ionization potential (IP), electron affinity (EA), electronegativity (χ), chemical potential (μ), electrophilicity index (ω), chemical hardness (η), and chemical softness (S). These parameters offer a deeper understanding of the electronic and chemical characteristics of the selected compounds **1g**, **1h**, **2b**, and **2d** [30]. The formulae used to calculate global chemical reactivity are listed in Eqs. (1–8).

$$E_{gap} = HOMO - LUMO \quad (1)$$

$$IP = -HOMO \quad (2)$$

$$EA = -LUMO \quad (3)$$

$$\chi = \frac{IP + EA}{2} \quad (4)$$

$$\eta = \frac{IP - EA}{2} \quad (5)$$

$$S = \frac{1}{2\eta} \quad (6)$$

$$\mu = \frac{-(IP + EA)}{2} \quad (7)$$

$$\omega = \frac{\mu^2}{2\eta} \quad (8)$$

3 Result and discussion

3.1 Synthetic optimisation

Vanillin azo precursors **1(a–h)** were synthesised following previously reported procedures [31], while vanillin azo-Schiff base hybrids **2(a–h)** were prepared *via* a condensation reaction between precursors **1(a–h)** and aniline in methanol under heating conditions, adapting a previously established methodology with slight modifications [18]. The synthetic method for obtaining target compounds is depicted in Scheme 1. The design strategy centred on the sequential synthesis of the compounds starting with the vanillin-azo moiety **1(a–h)**. This specific order is critical because the acidic conditions required for the diazo coupling reaction would otherwise cleave a pre-formed vanillin Schiff base [18, 32, 33]. The resulting vanillin-azo compound then serves as the scaffold for forming the vanillin azo Schiff base hybrids **2(a–h)**, ensuring the stable integration of both nitrogen functionalities.

The successful synthesis of **2(a–h)** were achieved using conventional heating in reflux conditions for 36 h, and the optimised yield was obtained using microwave irradiation. The conventional heating method by reflux for 36 h resulted in moderate yields of **2(a–h)** with 38–53%. Remarkably, microwave irradiation significantly improved 67–83% yield of **2(a–h)** with a shorter reaction time of 6 min at 170 °C (700 W). Microwave irradiation provided uniform and rapid heating throughout the reaction mixture, ensuring consistent reactions and higher yields [32, 33]. Moreover, MW irradiation minimised the tendency of the C = N bond to hydrolyse to form a side product due to the shorter reaction time, which could affect the yield [34–36]. Similar findings have been reported that water can hydrolyse the imine bonds induced by prolonged reaction *via* conventional heating [36, 37]. Microwave irradiation has been proven to shorten the reaction time, boost conversion and heighten selectivity [38]. The comparison for the percentage yield of **2(a–h)** using different methods is depicted in Fig. 2.

3.2 Spectral characterisation

Further analysis on FTIR, ¹H and ¹³C NMR explained the structures of the precursors **1(a–h)**, which corresponded to the previous literature [18]. The formation of compounds

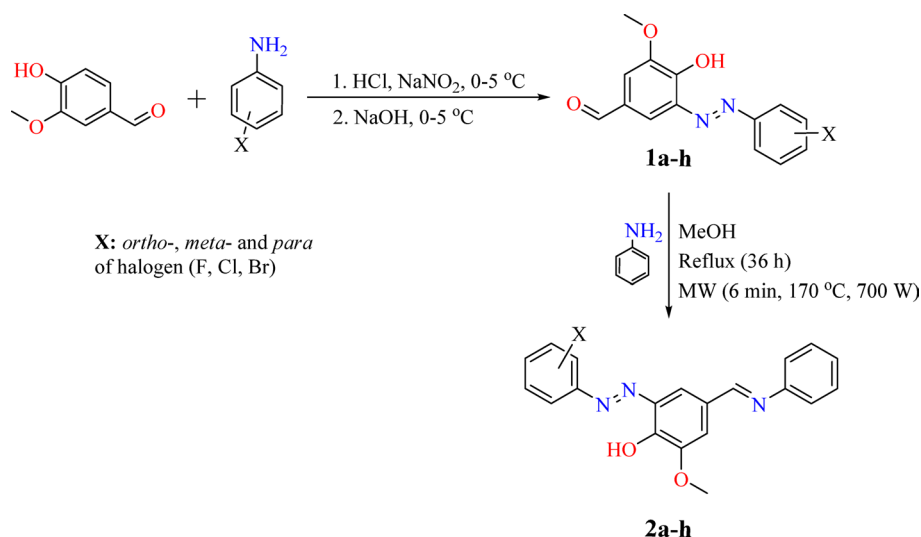


Fig. 1 Synthesis route of vanillin azo precursors **1(a–h)** and vanillin azo-Schiff base hybrids **2(a–h)**

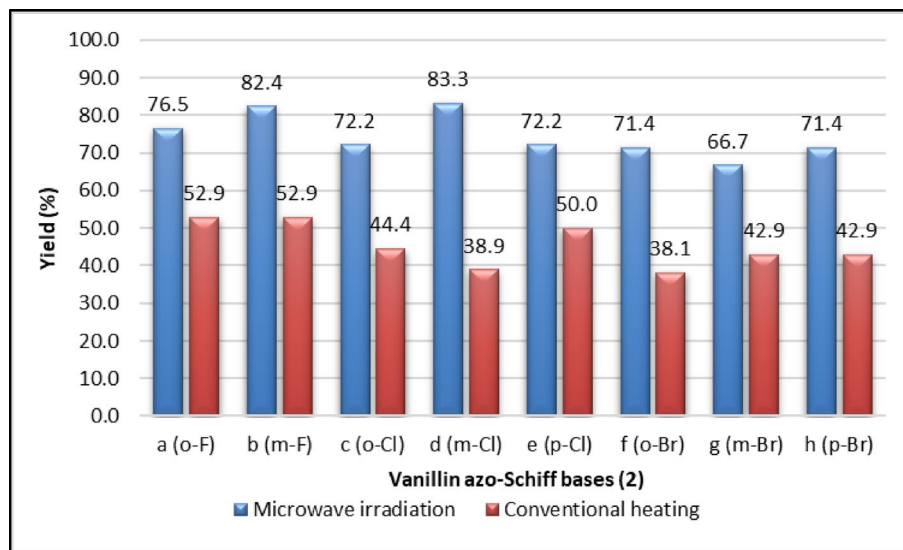


Fig. 2 Percentage yield of vanillin azo-Schiff base bearing halogen **2a–h** using microwave irradiation in comparison to conventional heating method

2(a–h) was confirmed by FTIR spectroscopy, evidenced by the disappearance of the carbonyl stretching vibration ($\nu(\text{C}=\text{O})$) in the range of $1649\text{--}1685\text{ cm}^{-1}$ [15] and the formation of a new absorption band at $1621\text{--}1625\text{ cm}^{-1}$, attributed to the imine stretching vibration ($\nu(\text{C}=\text{N})$). Other peaks such as $\nu(\text{N}=\text{N})$ and $\nu(\text{O}-\text{H})$ appeared at $1477\text{--}1492\text{ cm}^{-1}$ and $3425\text{--}3446\text{ cm}^{-1}$ on the FTIR spectra, respectively.

Apart from FTIR, ^1H NMR analysis was also conducted to prove the successful synthesis of **2(a–h)**, where compound **2e** was chosen to represent vanillin azo-Schiff base for comparison with vanillin azo precursor **1e**. ^1H NMR spectroscopy provided clear evidence that the vanillin azo-Schiff base has been formed. The disappearance of the aldehyde proton's singlet peak at 9.87 ppm in compound **1e** (H_7) and a new singlet at 8.55 ppm for compound **2e** has appeared, which corresponds to the imine's proton (H_7), confirming the successful synthesis of the hybrid compound (Fig. 3). The chemical shift of the aldehyde's proton appears further downfield compared to that of the imine proton, which can be attributed to the higher electronegativity of the oxygen atom relative to nitrogen, resulting in a greater deshielding effect [39]. Integration of the ^1H NMR spectrum revealed a resonance in the range of 7.18–8.05 ppm representing the eleven aromatic protons of compound **2e**. For ^{13}C NMR spectra, the disappearance of the carbonyl signal at 190.8–192.2.8.2 ppm (C_7) of **1e** and the emergence of a new peak at 160.3–164.3.3.3 ppm (C_7) were indicative of imine ($\text{C}=\text{N}$) formation of hybrid compound of **2e**.

3.3 Antibacterial evaluation (in vitro)

The antimicrobial efficacy of the synthesised compounds was initially assessed employing a turbidimetric kinetic procedure, specifically targeting *S. aureus* and *E. coli*. However, the compounds exhibited limited solubility, which is likely due to their inherent lipophilic nature [20]. This phenomenon resulted in the precipitation of the compounds and the formation of vehicle-insoluble particles within the culture medium, which could potentially interfere with the accurate assessment of antimicrobial activity [24, 40]. This outcome provides crucial insight into a key physicochemical property of these compounds, which is a significant consideration for their potential as drug candidates. As

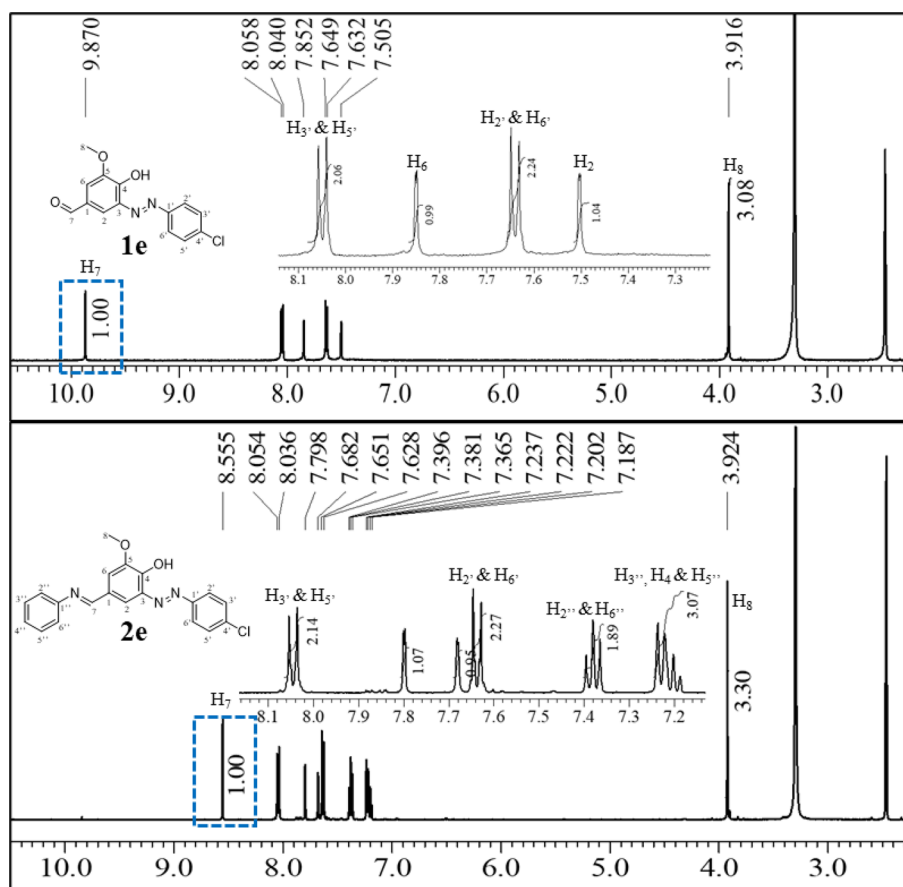


Fig. 3 ^1H NMR spectra of **1e** and **2e**

Table 1 Inhibition zone for in vitro antibacterial screening compounds **1(a-h)** and **2(a-h)**

Compound	Diameter of inhibition zone (mm)		Compound	Diameter of inhibition zone (mm)	
	<i>S. aureus</i>	<i>E. coli</i>		<i>S. aureus</i>	<i>E. coli</i>
1a (<i>o</i> -F)			2a (<i>o</i> -F)	11.10±0.10	10.10±0.10
1b (<i>m</i> -F)	9.03±0.15	8.03±0.15	2b (<i>m</i> -F)	11.20±0.10	11.03±0.12
1c (<i>o</i> -Cl)	8.07±0.15	8.10±0.17	2c (<i>o</i> -Cl)	9.07±0.06	10.07±0.15
1d (<i>m</i> -Cl)	8.03±0.12	–	2d (<i>m</i> -Cl)	10.07±0.15	10.07±0.06
1e (<i>p</i> -Cl)	–	–	2e (<i>p</i> -Cl)	10.03±0.12	8.10±0.10
1f (<i>o</i> -Br)	–	–	2f (<i>o</i> -Br)	11.17±0.06	8.00±0.17
1g (<i>m</i> -Br)	7.00±0.10	7.07±0.15	2g (<i>m</i> -Br)	9.17±0.12	9.17±0.06
1h (<i>p</i> -Br)	–	–	2h (<i>p</i> -Br)	10.03±0.12	9.17±0.12
Vanillin	–	–			
Ampicillin	12.23±0.15	10.23±0.15			

Used Disc=6 mm

an alternative approach, the antimicrobial efficacy of the target compounds was subsequently evaluated using the disc diffusion method, with the results summarised in Table 1; Fig. 4. The solubility limitations of the turbidimetric assay directly impact a compound's drug-likeness because a poorly soluble substance is unlikely to have sufficient bioavailability for it to be an effective drug in the body [41]. The assay's failure due to the few undissolved synthesised compounds interfering with the turbidity measurement was a valuable finding that highlighted a critical property of the molecules. The switch

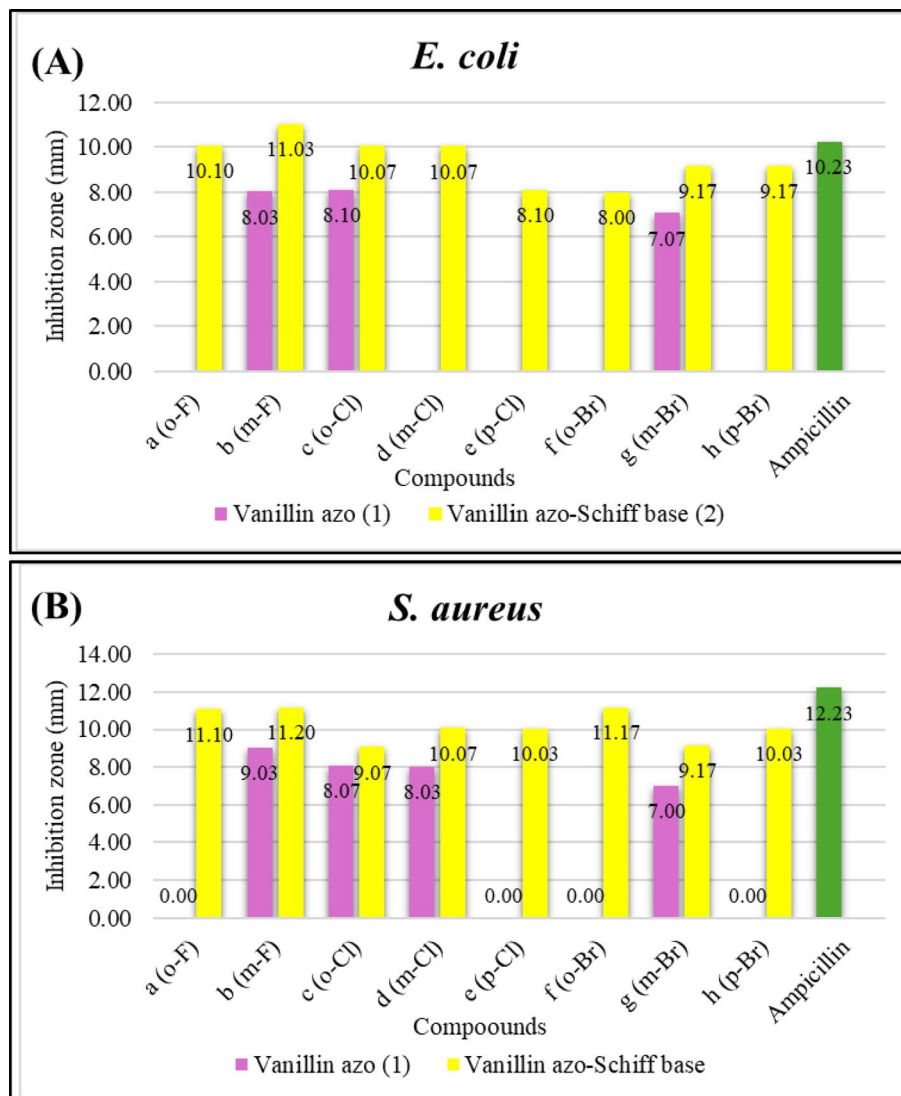


Fig. 4 Antibacterial activity of **1a–h** and **2a–h** against *E. coli* (A) and *S. aureus* (B)

to the disc diffusion method which relies on drug diffusion from a solid disc rather than full dissolution has successfully overcome this technical challenge and provided reliable data. This underscores the importance of a compound's physical properties for both effective testing and practical drug development.

Remarkably, compound **2(a–h)** demonstrated superior inhibition compared to **1(a–h)** against *E. coli* and *S. aureus*. This enhanced antibacterial property could be attributed to the synergistic effect of incorporating imine (C=N) and phenyl ring moieties onto vanillin azo **1(a–h)**, thus increasing the compound's hydrophilicity and lipophilicity. This finding aligned with previous research on hybrid azo-Schiff base compounds, which have shown excellent inhibition activity [21]. The formation of compounds **2(a–h)** by incorporating the Schiff base moiety into **1(a–h)** likely contributes to greater binding affinity and improved hydrogen bonding between synthesised compounds and the protein sites, which disrupts the growth of bacteria [42, 43]. The presence of a phenyl ring enhances a compound's lipophilic character, thereby facilitating its penetration through the thick outer membrane of bacteria [44].

Compound **2b** exhibited significant antibacterial activity, which is comparable to the standard ampicillin against both bacterial strains. The presence of the fluorine atom in compound **2b** is postulated to facilitate hydrogen bonding interactions, thereby enhancing its binding affinity and contributing to its efficacy in inhibiting bacterial cell proliferation [45]. Furthermore, the strategic *meta* position of the fluorine atom significantly contributed to favourable binding interactions with the bacterial surface, aligning with previous studies that highlight the impact of substituent position on biological properties [46, 47].

The enhanced antibacterial activity of the hybrid compounds **2(a–h)** can be attributed to the synergistic effect of their functional groups, namely azo (N=N), imine (C=N), hydroxyl (–OH), and methoxy (–OCH₃), which likely facilitate hydrogen bond interactions with biological receptors. These interactions may contribute to the superior efficacy of **2(a–h)** compared to compounds **1(a–h)**. This enhanced inhibition can also be attributed to the optimised balance of hydrophilic and lipophilic characteristics within the molecule [31, 48]. The inclusion of halogen atoms in the molecular structure has significantly improved the biological efficacy of the synthesised compounds *via* stabilisation of the non-hydrophobic interactions of the bacterium with halogen substituents. This effect is primarily achieved through the interaction of halogen bonding with the amino acid residues present in the bacterial environment [40].

3.4 Molecular docking analysis (in silico)

Docking simulations were conducted using the DNA gyrase B enzyme (PDB: 4URO) [49, 50] to evaluate the mode of interaction for ligands **2(a–b)** as antibacterial agents compared to moxifloxacin as a reference drug. Selecting this enzyme is crucial for developing drugs targeting its active sites, which are involved in the complex DNA winding and unwinding processes during bacterial replication and transcription [51]. The optimal binding site was determined using AutoGridFR [52], and the docking was analysed *via* AutoDock Vina [53, 54].

To validate the docking protocol implemented in AutoDock Vina, the crystal structure of the gyrase enzyme was re-docked to evaluate the reproducibility and reliability of the methodology. The re-docked inhibitor was subsequently superimposed onto the co-crystallised ligand within the original active site, yielding a root-mean-square deviation (RMSD) of 0.59 Å, within the acceptable threshold of 3.00 Å, indicating a reliable docking performance [55]. This result confirms that AutoDock Vina is a reliable tool for accurately predicting ligand–receptor interactions (Fig. 5).

The binding affinity and 3D interaction of **2(a–b)** are tabulated in Table 2. Both ligands **2a** and **2b**, which contain fluorine as substituents, demonstrated comparable binding affinities of –6.9 kcal/mol and –7.3 kcal/mol, respectively, relative to reference compound moxifloxacin (–7.7 kcal/mol). These findings agree with the *in vitro* data, further supporting the observed outcomes.

The ligand's influence on the target enzyme's physiological function improves with the increase of binding affinity or interaction intensity [56, 57]. Compared with moxifloxacin (Fig. 8), ligand **2(a–b)** can bind to multiple amino acid residues on the enzyme's active sites through different non-covalent interactions (Figs. 6 and 7). Various hydrophobic interactions, including amide- π , alkyl, π -alkyl and π - σ (represented by purple lines), can be observed between ligands **2a** and **2b** and the amino acid residues ASN54, GLY85,

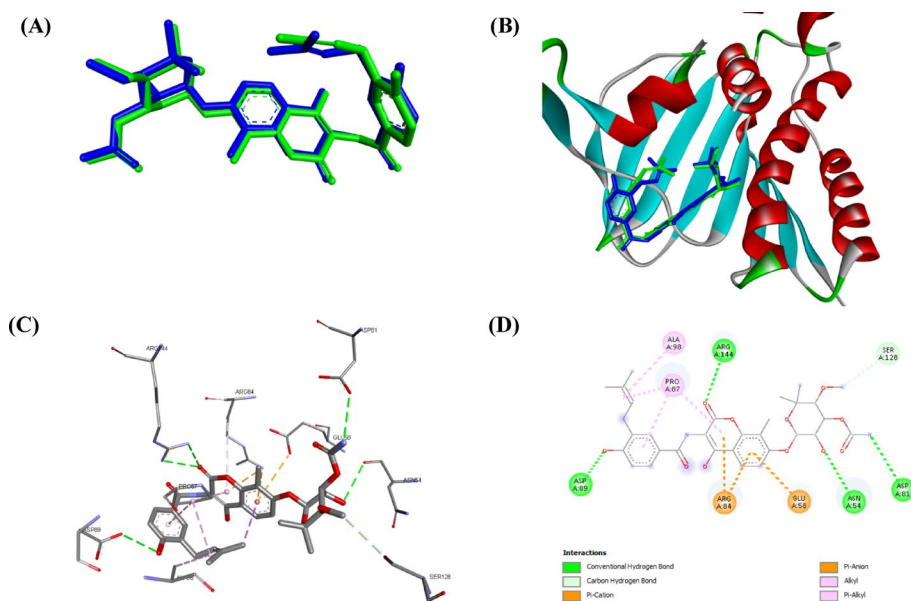


Fig. 5 **A** Superimposed of redocked (blue stick) and co-crystallised (green stick) inhibitors with RMSD of 0.59 Å. **B** Alignment of redocked (blue stick) and co-crystallised (green stick) inhibitors within the binding site of DNA gyrase enzyme. **C** 3D-complex structure of redocked ligand and protein receptor. **D** Visualisation of ligand-receptor interaction via 2D-complex structure

Table 2 Simulated Docking affinities and binding interaction residues

Ligand	Affinity (kcal/mol)	Interaction residues			
		Hydrogen	Halogen	Hydrophobic	Electrostatic
2a	- 6.9	ARG84, ARG144, GLY85	ARG84, ARG144	GLY85, ILE86, ILE102, PRO87	GLU58
2b	- 7.3	SER128, VAL126	-	ASN54, GLY85, ILE86, ILE102, PRO87, SER55, VAL105	-
Moxifloxacin	- 7.7	ASP81, THR173	GLU58, GLY85	ASN54, GLY85, PRO87, ILE86	GLU58

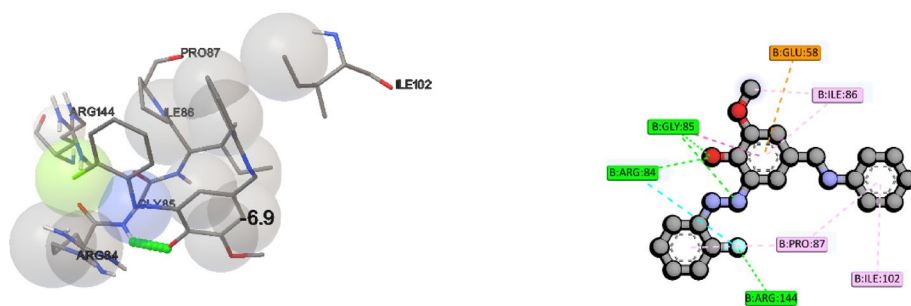


Fig. 6 3D and 2D binding modes of **2a** in the active site of DNA gyrase enzyme

ILE86, ILE102, PRO87, SER55 and VAL105. This is due to the presence of various active pharmacophores such as Schiff base, azo, fluorine and aromatic groups onto vanillin, which increased the ligand lipophilic characteristic for hydrophobic interactions, enhancing the binding affinity and antibacterial potential of the compounds [58].

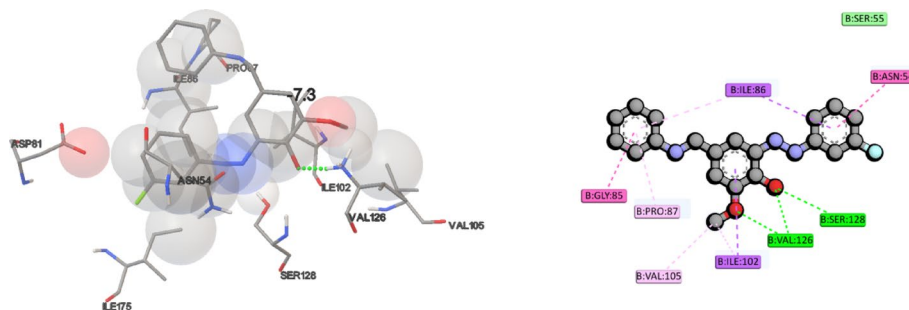


Fig. 7 3D and 2D binding modes of **2b** in the active site of DNA gyrase enzyme

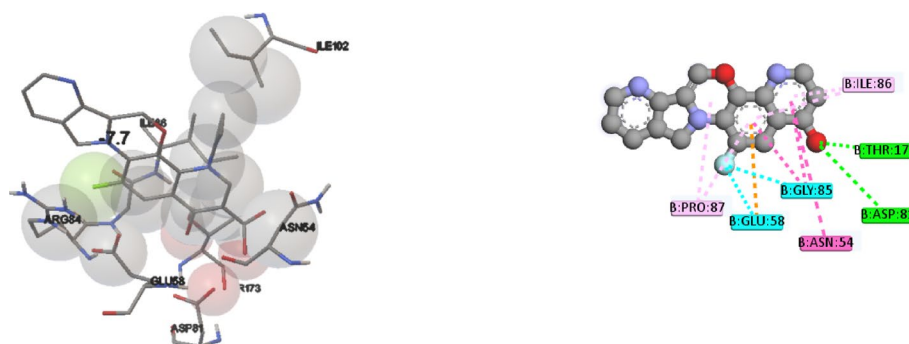


Fig. 8 3D and 2D binding modes of moxifloxacin in the active site of DNA gyrase enzyme

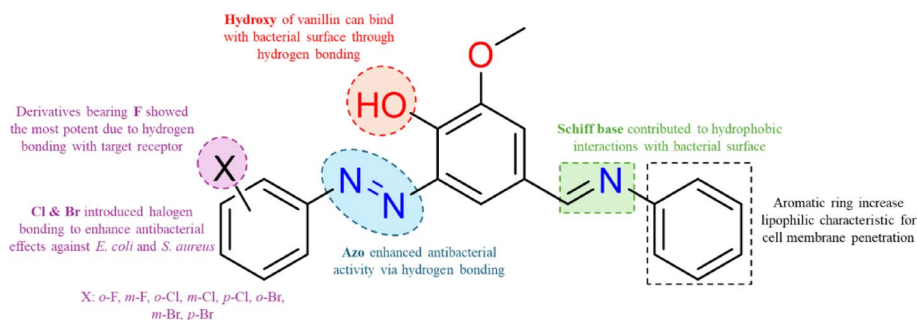
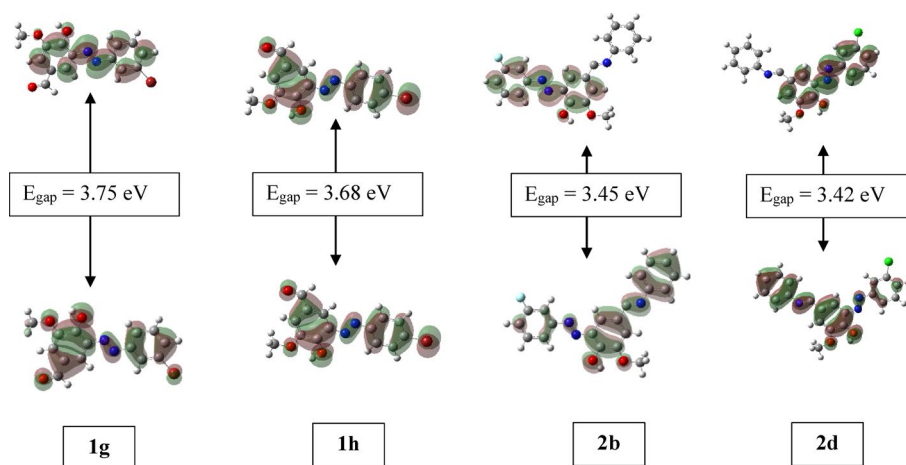


Fig. 9 SAR of halogenated vanillin azo-Schiff base

The strong ligand-enzyme interactions of **2(a-b)** were also influenced by their ability to form multiple hydrogen bond interactions between ARG84, ARG144, GLY85, SER128 and VAL126 residues through azo, hydroxyl and fluorine atoms, similar to moxifloxacin. This hydrogen bonding helps to stabilise the formation of the ligand-enzyme complex, thus preventing the enzyme function [59, 60]. The presence of a fluorine atom actively contributed to the ligand-enzyme interaction by forming halogen bond interactions with ARG84 and ARG144. Its high electronegativity simultaneously enhanced the ligand's lipophilicity and facilitated hydrogen bond interactions, collectively optimising the binding affinity [45, 61]. In addition, ligands **2(a-b)** replicate the moxifloxacin binding interaction with GLY85, PRO87, and ILE86 residues, showing a comparable inhibitory mode of action. The structure-activity Relationship (SAR) studies of the hybrid vanillin azo-Schiff base with the biological target have been illustrated in Fig. 9.

Table 3 Measurement of global chemical reactivity descriptors using B3LYP/6-311G (d, p) method

	1g (m-Br)	1h (p-Br)	2b (m-F)	2d (m-Cl)
EHOMO (eV)	-6.46	-6.37	-5.98	-6.00
ELUMO (eV)	-2.71	-2.69	-2.53	-2.58
E_{gap} (eV)	3.75	3.68	3.45	3.42
Ionization potential (IP)	6.46	6.37	5.98	6.00
Electron affinity (EA)	2.71	2.69	2.53	2.58
Electronegativity (X)	4.59	4.53	4.26	4.29
Chemical potential (μ)	-4.59	-4.53	-4.26	-4.29
Chemical hardness (η)	1.88	1.84	1.73	1.71
Electrophilic index (w)	5.60	5.58	5.24	5.38
Chemical softness (S)	0.27	0.27	0.29	0.29

**Fig. 10** Energy level diagram of the synthesized compounds

3.5 DFT study

The electronic structure and reactivity of the compounds were evaluated using Density Functional Theory (DFT) and are presented in Table 3. The Highest Occupied Molecular Orbital (HOMO) and Lowest Unoccupied Molecular Orbital (LUMO) energy levels, which reflect the molecules' electron-donating and electron-accepting capabilities, were calculated for **1g**, **1h**, **2b**, and **2d**. The HOMO-LUMO energy gap (E_{gap}) serves as a key indicator of chemical reactivity, with a smaller gap signifying a more reactive molecule [62]. For example, compound **2b**, which exhibits superior antibacterial activity among the synthesised compounds, produces a smaller E_{gap} (3.45 eV). This analysis indicates that the increased reactivity is a crucial factor in their mechanism of action against bacterial pathogens (Fig. 10) [63].

Furthermore, the chemical hardness of the target compounds in the range of 1.71–1.88 eV corresponds to the properties of molecules resistant to electron exchange. In contrast, the chemical softness of the compounds highlights their potential to respond to external perturbations, with hybrid compounds **2b** and **2d** exhibiting higher chemical softness values compared to the vanillin azo precursors **1g** and **1h**. The molecules' electron affinity and polarizability contribute to electronegativity values ranging from 4.26 to 4.59 eV.

Moreover, the synthesised compounds are ready for electron acceptance with electrophilicity indices of 5.24 to 5.60 (eV) during the occurrence of the chemical reaction.

DFT calculations reveal notable patterns where the low electronegativity of **2b** displays a unique weakened electron affinity that determines its characteristics. With the smallest electrophilicity index, compound **2b** exhibits a distinct reduced electrophilicity. The electronic potential of the synthesised compounds significantly highlights their electron-donation tendencies. The significant chemical hardness and molecular softness values of the synthesised compounds indicate their insusceptibility towards the donation of electrons and remarkable response to perturbations, respectively [64].

3.6 Pharmacokinetic studies

The promising in vitro antibacterial activity supported by the in silico docking and DFT studies was further complemented by favourable pharmacokinetic properties, which are essential for a successful drug candidate. All compounds were analysed for their ADMET profile and pharmacokinetic properties using SwissADME and pkCSM online tools (Table S3 and S4). According to pharmacokinetic studies, all synthesised compounds data suggested favourable drug-likeness, good bioavailability and potential for oral administration. Key properties like Lipinski's Rule compliance and low toxicity contributed to enhancing its therapeutic viability [65]. None of the compounds violates any established rules, and a standard bioavailability score (ABS) of 0.55 was calculated. The synthetic accessibility ranged from 2.48 to 3.32, in compliance with Lipinski's rule. All compounds demonstrated excellent human intestinal absorption (HIA), ranging from 84.335% to 91.545%. The compounds exhibited Log BB values between -0.691 and 0.302 , and log PS values from -2.133 to -1.428 , indicating effective drug distribution to the brain and potential CNS penetration.

All compounds exhibited a strong potential for crossing biological barriers [27], as presented in Table S2. Drug biotransformation was assessed through enzymatic metabolism, with cytochrome P450 enzymes playing a key role, particularly the CYP families 1A2, 2C9, 2C19, 2D6, and 3A4. Notably, CYP3A4 functions as both a substrate and an inhibitor. Total clearance, which reflects the rate of drug elimination relative to its concentration in the body, is considered moderate to high when values exceed 5–15. All compounds meet the acceptable criteria for drug clearance, with values ranging from -0.664 to 0.291 [65].

4 Conclusions

In conclusion, compounds **2(a–h)** were successfully synthesised with improved yields upon microwave irradiation compared to conventional heating methods. The antibacterial evaluation of the hybrid vanillin derivatives containing azo ($-N=N$) and imine ($-C=N$) functionalities **2(a–h)** revealed excellent antimicrobial effects against *E. coli* and *S. aureus*, surpassing the efficacy of both the parent vanillin and vanillin azo precursors **1(a–h)**. The hybridisation of azo and Schiff base functionalities through vanillin as a linker facilitated synergistic effects, strengthening the ligand's interactions with the bacterial surface. Compound **2b** demonstrated the most potent antibacterial activity among the synthesised compounds, which is well-correlated with its strong docking affinity of -7.3 kcal/mol and a relatively low HOMO-LUMO energy gap of 3.45 eV. These parameters collectively suggest an optimal balance of reactivity and molecular stability, facilitating effective interaction with the biological target. The promising ADMET properties make these hybrid compounds good candidates for further drug development. These

collective findings underscore the considerable potential of the hybrid compounds in offering innovative strategies for the effective treatment of bacterial infections. To fully achieve this potential, future research is encouraged to integrate detailed computational studies (i.e. MEP analysis with comprehensive biological evaluations) including cytotoxicity assays, in vitro broader-spectrum antibacterial testing and in vivo evaluations to establish pharmacokinetic profiles and safety toward clinical relevance.

Supplementary Information

The online version contains supplementary material available at <https://doi.org/10.1007/s42452-025-07929-8>.

Supplementary Material 1.

Acknowledgements

The authors express their gratitude to Universiti Malaysia Sarawak for the financial support through UNIMAS Graduate Research Grant.

Author contributions

Z. and M.A. were responsible for the conceptualisation, research design, and acquisition of funding. M.A. conducted the synthesis, characterisation, and in vitro studies. In silico molecular docking, Density Functional Theory (DFT) calculations and ADMET analysis were performed by N.A., A.I., and S., respectively. M.A., N.A., A.I., and S. collaboratively prepared the original manuscript draft and supplementary materials. Z. reviewed and edited the manuscript. All authors reviewed the manuscript.

Funding

Open Access funding provided by Universiti Malaysia Sarawak. The work is funded by UNIMAS Graduate Research Grant: UNI/F07/GRADUATE/86747/2025.

Data availability

All data supporting the findings presented in this study are accessible within the main paper and its associated supplementary information files.

Declarations

Ethics approval and consent to participate

Not applicable.

Consent for publication

Not applicable.

Competing interests

The authors declare no competing interests.

Received: 26 July 2025 / Accepted: 29 October 2025

Published online: 26 November 2025

References

- Ikuta KS, et al. Global mortality associated with 33 bacterial pathogens in 2019: a systematic analysis for the global burden of disease study 2019. *Lancet*. 2022;400(10369):2221–48. [https://doi.org/10.1016/S0140-6736\(22\)02185-7](https://doi.org/10.1016/S0140-6736(22)02185-7).
- Ngaini Z, Mortadza NA. Synthesis of halogenated azo-aspirin analogues from natural product derivatives as the potential antibacterial agents. *Nat Prod Res*. 2019;33(24):3507–14. <https://doi.org/10.1080/14786419.2018.1486310>.
- Ngaini Z, Rasin F, Wan Zulkiplee WSH, Abd Halim AN. Synthesis and molecular design of mono aspirinate thiourea-azo hybrid molecules as potential antibacterial agents. *Phosphorus Sulfur Silicon Relat Elem*. 2020;196(3):275–82. <https://doi.org/10.1080/10426507.2020.1828885>.
- Raymond Mohanraj DG, Alagumuthu M, Subramaniam P, Bakthavachalam D, Arumugam S, Chellam S. Antimicrobial effects of vanillin-based pyridyl-benzylidene-5-fluoroindolins. *J Heterocycl Chem*. 2021;58(7):1515–24. <https://doi.org/10.1002/jhet.4277>.
- Anand A, Wahal N, Mehta M, Satija S. Vanillin: a comprehensive review of pharmacological activities. *Plant Arch*. 2019;19(2):1000–4.
- Mortadza NA, Ngaini Z. Microwave-assisted and conventional synthesis of halogenated coumarin-azo derivatives and structural-activity relationship study for antimicrobial potential. *Malaysian J Anal Sci*. 2023;27(2):342–52.
- Gulsia O. Vanillin: one Drug, many cures. *Resonance*. 2020;25(7):981–6.
- Li M, Lang Y, Gu M, Shi J, Chen BPC, Yu L. Vanillin derivative VND3207 activates DNA-PKcs conferring protection against radiation-induced intestinal epithelial cells injury in vitro and in vivo. *Toxicol Appl Pharmacol*. 2020;387(2019):114855. <https://doi.org/10.1016/j.taap.2019.114855>.
- Ma W, et al. IPM712, a vanillin derivative as potential antitumor agents, displays better antitumor activity in colorectal cancers cell lines. *Eur J Pharm Sci*. 2020;152:105464. <https://doi.org/10.1016/j.ejps.2020.105464>.

10. Singh G, et al. Bis-Schiff base for selective detection of Al(III) and citric acid: Real sample analysis, anticancer potential and docking study. *Inorganica Chim Acta*. 569:122148. <https://doi.org/10.1016/j.ica.2024.122148>.
11. Hariono M, Abdullah N, Damodaran KV, Kamarulzaman EE, Nat Publ Gr. Potential new H1N1 neuraminidase inhibitors from ferulic acid and vanillin: molecular modelling, synthesis and in vitro assay. *Sci Rep*. 2016(1). <https://doi.org/10.1038/srep38692>.
12. Kim JH, et al. A vanillin derivative causes mitochondrial dysfunction and triggers oxidative stress in *Cryptococcus neoformans*. *PLoS One*. 2014;9(2):e89122. <https://doi.org/10.1371/journal.pone.0089122>.
13. Patrick CA, Webb JP, Green J, Chaudhuri RR, Collins MO, Kelly DJ. Proteomic profiling, transcription factor modeling, and genomics of evolved tolerant strains elucidate mechanisms of vanillin toxicity in *Escherichia coli*. *Appl Environ Sci*. 2019;4(4):1–29. <https://doi.org/10.1128/msystems.00163-19>.
14. Pagariya SK, Pathade RM, Boddhe PS. Synthesis, characterization and antimicrobial screening of some azo compounds derived from ethyl vanillin. *Res J Chem Sci*. 2015;5(7):20–8.
15. Ngaini Z, Hissam MA, Mortadza NA, Abd Halim AN, Daud AI. In vitro antimicrobial activities, molecular docking and density functional theory (DFT) evaluation of natural product-based Vanillin derivatives featuring halogenated Azo dyes. *Nat Prod Res*. 2023;38(21):3762–72. <https://doi.org/10.1080/14786419.2023.2262713>.
16. Chigurupati S. Designing new Vanillin schiff bases and their antibacterial studies. *J Med Bioeng*. 2015;4(5):363–6. <https://doi.org/10.12720/jomb.4.5.363-366>.
17. Sobola A. Synthesis, characterization and antimicrobial activity of p-Vanillin and Vanillin schiff bases. *J Res Rev Sci*. 2018;5(1):51–7. [https://doi.org/10.36108/jrslasu/8102/50\(0160\)](https://doi.org/10.36108/jrslasu/8102/50(0160)).
18. Hissam MA, Ngaini Z, Zamakshari NH, Hejemi FNAM, Arni FS, Halim ANA. Synthesis and molecular docking simulation on the antimicrobial effects of halogenated vanillin-azo dyes and schiff base derivatives. *Discov Appl Sci*. 2024;6(6):325. <https://doi.org/10.1007/s42452-024-05830-4>.
19. Adu JK, et al. Synthesis and in vitro antimicrobial and anthelmintic evaluation of naphtholic and phenolic azo dyes. *J Trop Med*. 2020;2020:1–8. <https://doi.org/10.1155/2020/4850492>.
20. Hassan AS, Hafez TS, Osman SAM, Ali MM. Synthesis and in vitro cytotoxic activity of novel pyrazolo[1,5-a]pyrimidines and related schiff bases. *Turkish J Chem*. 2015;39(5):1102–13. <https://doi.org/10.3906/kim-1504-12>.
21. Kaur H, Lim SM, Ramasamy K, Vasudevan M, Shah SAA, Narasimhan B. Diazenyl schiff bases: Synthesis, spectral analysis, antimicrobial studies and cytotoxic activity on human colorectal carcinoma cell line (HCT-116). *Arab J Chem*. 2020;13(1):377–92. <https://doi.org/10.1016/j.arabc.2017.05.004>.
22. Leonard E, Takeda C, Akitsu T. Azobenzene-containing Schiff-bases—syntheses and dyes applications. *Colorants*. 2024;3(1):53–72. <https://doi.org/10.3390/colorants3010004>.
23. Hissam MA, Ngaini Z, Patrick Mesebasio SI, Jeffrey Shahren DA. Synthesis, antibacterial, antioxidant, molecular docking and ADMET properties of halogenated vanillin azo-chalcone. *Discov Appl Sci*. 2025;7(7):654. <https://doi.org/10.1007/s42452-025-07252-2>.
24. Farooq S, Ngaini Z. Synthesis, molecular docking and antimicrobial activity of α , β -unsaturated ketone exchange moiety for chalcone and pyrazoline derivatives. *ChemSelect*. 2020;5(32):9974–9. <https://doi.org/10.1002/slct.202002278>.
25. Daina A, Michieli O, Zoete V. SwissADME: a free web tool to evaluate pharmacokinetics, drug-likeness and medicinal chemistry friendliness of small molecules. *Sci Rep*. 2017;7(1):42717. <https://doi.org/10.1038/srep42717>.
26. Pires DEV, Blundell TL, Ascher DB. pkCSM: predicting small-molecule pharmacokinetic and toxicity properties using graph-based signatures. *J Med Chem*. 2015;58(9):4066–72. <https://doi.org/10.1021/acs.jmedchem.5b00104>.
27. Chagas CM, Moss S, Alisarai L. Drug metabolites and their effects on the development of adverse reactions: revisiting lipinski's rule of five. *Int J Pharm*. 2018;549(1–2):133–49. <https://doi.org/10.1016/j.ijpharm.2018.07.046>.
28. Frisch MJ, et al. Gaussian 09 W, revision A. 02., 2009.
29. Dennington R, Keith T, Millam J. GaussView, version 5. 2009.
30. Arzine A, et al. Design, synthesis, in-vitro, in-silico and DFT studies of novel functionalized isoxazoles as antibacterial and antioxidant agents. *Comput Biol Chem*. 2024;108:107993.
31. Ngaini Z, Hissam MA, Mortadza NA, Abd Halim AN, Daud AI. In vitro antimicrobial activities, molecular docking and density functional theory (DFT) evaluation of natural product-based Vanillin derivatives featuring halogenated azo dyes. *Nat Prod Res*. 2023;38(21):1–11. <https://doi.org/10.1080/14786419.2023.2262713>.
32. Gupta D, Jamwal D, Rana D, Katoch A. Microwave synthesized nanocomposites for enhancing oral bioavailability of drugs. *Appl Nanocomposite Mater Drug Deliv*. 2018. <https://doi.org/10.1016/B978-0-12-813741-3.00027-3>.
33. Makwana S, Kumari P. Microwave assisted synthesis: a green chemistry approach and future directions. *Futur Green Synth*. 2023;5:1–60.
34. Pramanik B, Das D. Aggregation-induced emission or hydrolysis by water? The case of schiff bases in aqueous organic solvents. *J Phys Chem C*. 2018;122(6):3655–61. <https://doi.org/10.1021/acs.jpcc.7b12430>.
35. Sharma P, Tripathi A, Tripathi PN, Sen Singh S, Singh SP, Shrivastava SK. Novel molecular hybrids of N-benzylpiperidine and 1,3,4-oxadiazole as multitargeted therapeutics to treat Alzheimer's disease. *ACS Chem Neurosci*. 2019;10(10):4361–84. <https://doi.org/10.1021/acschemneuro.9b00430>.
36. Barmatov E, Hughes T. Degradation of a schiff-base corrosion inhibitor by hydrolysis, and its effects on the Inhibition efficiency for steel in hydrochloric acid. *Mater Chem Phys*. 2021;257(3):123758. <https://doi.org/10.1016/j.matchemphys.2020.123758>.
37. Misra P, Mishra BK, Behera GB. Hydrolysis of schiff bases, 1: kinetics and mechanism of spontaneous, acid, and base hydrolysis of N-(2/4-hydroxybenzylidene)-2-aminobenzothiazoles. *Int J Chem Kinet*. 1991;23(7):639–54. <https://doi.org/10.1002/kin.550230709>.
38. Shalaby MA, Fahim AM, Rizk SA. Microwave-assisted synthesis, antioxidant activity, docking simulation, and DFT analysis of different heterocyclic compounds. *Sci Rep*. 2023;13(1):4999. <https://doi.org/10.1038/s41598-023-31995-w>.
39. Dong X, Oganov AR, Cui H, Zhou XF, Wang HT. Electronegativity and chemical hardness of elements under pressure. *Proc Natl Acad Sci U S A*. 2022;119(10):1–8. <https://doi.org/10.1073/pnas.2117461119>.
40. Abd Halim AN, Ngaini Z. Synthesis and characterization of halogenated bis(acylthiourea) derivatives and their antibacterial activities. *Phosphorus Sulfur Silicon Relat Elem*. 2017;192(9):1012–7. <https://doi.org/10.1080/10426507.2017.1315421>.
41. Bhalani DV, Nutan B, Kumar A, Singh Chandel AK. Bioavailability enhancement techniques for poorly aqueous soluble drugs and therapeutics. *Biomedicines*. 2022;10(9):2055. <https://doi.org/10.3390/biomedicines10092055>.

42. Jadama A, Yuksekdanaci S, Astley D, Yasa I. Synthesis, characterization and biological activity of schiff and Azo-Schiff base ligands. *Stud Univ Babeş-Bolyai Chem.* 2023;2023(1):75–89. <https://doi.org/10.24193/subbchem.2023.1.06>.
43. Muhammad-Ali MA, Jasim EQ, Al-Saadon AH. Synthesis, antibacterial Evaluation, and Docking studies of some Azo compounds and schiff bases derived from sulfonamide. *J Med Chem Sci.* 2023;6(9):2128–39. <https://doi.org/10.26655/JMCHEMSCI.2023.9.19>.
44. Zgurskaya HI, López CA, Gnanakaran S. Permeability barrier of Gram-negative cell envelopes and approaches to bypass it. *ACS Infect Dis.* 2015;1(11):512–22. <https://doi.org/10.1021/acsinfecdis.5b00097>.
45. Dalvit C, Invernizzi C, Vulpetti A. Fluorine as a hydrogen-bond acceptor: experimental evidence and computational calculations. *Chem Eur J.* 2014;20:11058–68. <https://doi.org/10.1002/chem.201402858>.
46. Kosikowska U, Wujec M, Trotsko N, Plonka W, Paneth P, Paneth A. Antibacterial activity of fluorobenzoylthiosemicarbazides and their Cyclic analogues with 1,2,4-triazole scaffold. *Molecules.* 2021;26(1):1–18. <https://doi.org/10.3390/MOLECULES26010170>.
47. Nordin NA, et al. In vitro cytotoxicity evaluation of thiourea derivatives bearing *Salix* sp. constituent against HK-1 cell lines. *Nat Prod Res.* 2020;34(11):1505–14. <https://doi.org/10.1080/14786419.2018.1517120>.
48. Gull P, Hashmi AA. Biological activity studies on metal complexes of macrocyclic schiff base ligand: synthesis and spectroscopic characterization. *J Braz Chem Soc.* 2015;26(7):1331–7. <https://doi.org/10.5935/0103-5053.20150099>.
49. Amer HH, Eldrehmy EH, Abdel-Hafez SM, Alghamdi YS, Hassan MY, Alotaibi SH. Antibacterial and molecular Docking studies of newly synthesized nucleosides and schiff bases derived from sulfadimidines. *Sci Rep.* 2021;11(1):1–14. <https://doi.org/10.1038/s41598-021-97297-1>.
50. Gupta M, Sharma R, Kumar A. Comparative potential of Simvastatin, Rosuvastatin and Fluvastatin against bacterial infection: an in silico and in vitro study. *Orient Pharm Exp Med.* 2019;19(3):259–75. <https://doi.org/10.1007/s13596-019-00359-z>.
51. Rahimi H, Najafi A, Eslami H, Negahdari B, Moghaddam MM. Identification of novel bacterial DNA gyrase inhibitors: an in silico study. *Res Pharm Sci.* 2016;11(3):233–42.
52. Ravindranath PA, Forli S, Goodsell DS, Olson AJ, Sanner MF. AutoDockFR: advances in Protein-Ligand Docking with explicitly specified binding site flexibility. *PLoS Comput Biol.* 2015;11(12):1–28. <https://doi.org/10.1371/journal.pcbi.1004586>.
53. Eberhardt J, Santos-Martins D, Tillack AF, Forli S. Autodock Vina 1.2.0: new docking methods, expanded force field, and python bindings. *J Chem Inf Model.* 2021;61(8):3891–8. <https://doi.org/10.1021/acs.jcim.1c00203>.
54. Trott O, Olson AJ. AutoDock vina: improving the speed and accuracy of Docking with a new scoring function, efficient optimization, and multithreading. *J Comput Chem.* 2010;31(2):455–61.
55. Abd Halim AN, Yeo KW, Zamakshshari NH, Phornvillay S, Ngaini Z, Diosing DN. Preparation, in vitro and in Silico antioxidant and antibacterial studies of 4-aminoacetanilide Azo derivatives. *J Indian Chem Soc.* 2024;101(11):101341. <https://doi.org/10.1016/j.jics.2024.101341>.
56. Seo S, Choi J, Park S, Ahn J. Binding affinity prediction for protein–ligand complex using deep attention mechanism based on intermolecular interactions. *BMC Bioinformatics.* 2021. <https://doi.org/10.1186/s12859-021-04466-0>.
57. Farinde A. Drug–receptor interactions. 2022. <https://www.msmanuals.com/professional/clinical-pharmacology/pharmacodynamics/drug-receptor-interactions>
58. Patil R, Das S, Stanley A, Yadav L, Sudhakar A, Varma AK. Optimized hydrophobic interactions and hydrogen bonding at the target-ligand interface leads the pathways of drug-designing. *PLoS One.* 2010. <https://doi.org/10.1371/journal.pone.0012029>.
59. Kumar A, Prasun C, Rathi E, Nair MS, Kini SG. Identification of potential DNA gyrase inhibitors: virtual screening, extra-precision docking and molecular dynamics simulation study. *Chem Pap.* 2023;77(11):6717–27. <https://doi.org/10.1007/s11696-023-02971-5>.
60. Ghannam IAY, Abd El-Meguid EA, Ali IH, Sheir DH, El AM, Kerdawy. Novel 2-arylbenzothiazole DNA gyrase inhibitors: Synthesis, antimicrobial evaluation, QSAR and molecular Docking studies. *Bioorg Chem.* 2019;93:103373. <https://doi.org/10.1016/j.bioorg.2019.103373>.
61. Jeschke P. The unique role of halogen substituents in the design of modern agrochemicals. *Pest Manag Sci.* 2010;66(1):10–27. <https://doi.org/10.1002/ps.1829>.
62. Belay Y, et al. Molecular hybrid of 1, 2, 3-triazole and schiff base as potential antibacterial agents: DFT, molecular docking and ADME studies. *J Mol Struct.* 2023;1286:135617.
63. Elangovan N, Alomar SY, Sowrirajan S, Rajeswari B, Nawaz A, Kalanthoden AN. Photoluminescence property and solvation studies on (E)-N-(pyrimidin-2-yl)-4-((3,4,5-trimethoxy benzylidene) amino) benzene sulfonamide; Synthesis, structural, topological analysis, antimicrobial activity and molecular Docking studies. *Inorg Chem Commun.* 2023;155(6):111019. <https://doi.org/10.1016/j.inoche.2023.111019>.
64. Patel M, Kikani T, Patel K, Thakore S. Synthesis, characterization and DFT studies of novel schiff base derivatives of Curcumin as potential antibacterial agents. *J Mol Struct.* 2024;1295:136691.
65. Ahmad I, Kuznetsov AE, Pirzada AS, Alsharif KF, Daglia M, Khan H. Computational pharmacology and computational chemistry of 4-hydroxyisoleucine: physicochemical, pharmacokinetic, and DFT-based approaches. *Front Chem.* 2023. <https://doi.org/10.3389/fchem.2023.1145974>.

Publisher's note

Springer Nature remains neutral with regard to jurisdictional claims in published maps and institutional affiliations.